Nuclear Engineering and Design 240 (2010) 763–770

Contents lists available at ScienceDirect

Nuclear Engineering and Design

journal homepage: www.elsevier.com/locate/nucengdes

FMSR: A code system for in-core fuel management calculation of aqueous homogeneous solution reactor

Yunzhao Li[a], Hongchun Wu[a], Liangzhi Cao[a,*], Qichang Chen[a], Haoliang Lu[a], Sitao Peng[a], Xiaoming Song[b], Dong Yao[b]

[a] School of Nuclear Science and Technology, Xi'an Jiaotong University, 28, Xianning West Road, Xi'an, Shaanxi 710049, China
[b] State Key Lab of Reactor System Design Technology, Nuclear Power Institute of China, Chengdu 610041, China

ARTICLE INFO

Article history:
Received 26 February 2009
Received in revised form 2 September 2009
Accepted 13 October 2009

ABSTRACT

Aqueous homogeneous solution reactor is a promising concept for the production of medical isotopes. But some characteristics of aqueous solution reactors, such as no traditional assembly in the core, the gas bubbles' generation in fuel solution, isotopes distillation, unstructured geometry, strong anisotropic scattering, etc., make the fuel management calculation very complicated. This study establishes a suitable calculation model for aqueous homogeneous solution reactors and developed an in-core fuel management calculation code FMSR (Fuel Management for Solution Reactors) based on the 3D transport solver DNTR. Numerical results indicate that FMSR can be used for the fuel management calculation of homogeneous aqueous solution reactor as a trial.

1. Introduction

Other than the irradiation of uranium targets in heterogeneous reactors, aqueous homogeneous solution reactors present an alternative way to produce medical isotopes. Based on many potential advantages of aqueous homogeneous solution reactors (Souto et al., 2005), the Medical Isotope Production Reactor (MIPR) concept has been proposed for the production of medical isotopes (Ball, 1997).

However, there are a lot of inconveniences in the fuel management calculation of aqueous homogeneous solution reactors. First, there are no assemblies in the core which is very different from the traditional reactor core. For example, the structure of the object in this work is shown in Fig. 1. Second, the operation of aqueous solution reactor at a power of 200 kW will generate radiolytic-gas bubbles (Souto et al., 2005). The void volume created by these bubbles in the solution core will introduce a strong negative reactivity feedback. Third, the small volume and strong anisotropic scattering of the reactor core make the diffusion theory inapplicable, and neutron transport theory is required. Fourth, the complex structure of the coolant pipes immersed in fuel solution requires unstructured neutron transport calculation methods. Fifth, the distillation of isotopes makes fuel management calculation more complicated than traditional solid-fuel reactors.

Several assemblies have been developed, such as KEWB (Dunenfeld and Stitt, 1963), CRAC (Lecorche and Seale, 1973), and SHEBA (Malenfant et al., 1980), etc. But they are used in criticality safety research and no special report on aqueous homogeneous solution reactor's fuel management calculation has been found until now.

Considering the characteristics of aqueous homogeneous solution reactors, this work establishes a suitable calculation model for the fuel management calculation of these reactors and develops a code named FMSR based on the code DNTR (Lu, 2007), a 3D S_N nodal transport calculation code for triangular-z meshes. The calculation model is introduced in Section 2. Numerical results are presented in Section 3 and conclusions in Section 4.

2. Calculation model

As the direct heterogeneous calculation for whole core is quite time consuming, the physics calculation of aqueous homogeneous solution reactors is divided into two steps, namely, the few-group homogeneous constants calculation and the 3D in-core fuel management calculation.

On one hand, there are no assemblies in the core. As a result, the core should be divided into some regions for homogenization. In this paper, the compartmentalization of the 1/6 core, as shown in Fig. 2 has been used because of the symmetry. On the other hand, in order to save time, 2D transport calculation and 1D fundamental mode modification have been implemented in few-group constants calculation. In this work, fundamental mode calculation is performed in 1-dimension, 69 energy groups with P1 approximation. And the corresponding relationship between homogenization and in-core calculation is also shown in Fig. 2.

* Corresponding author. Tel.: +86 29 82663285; fax: +86 29 82667802.
E-mail address: caolz@mail.xjtu.edu.cn (L. Cao).

0029-5493/$ – see front matter © 2009 Elsevier B.V. All rights reserved.
doi:10.1016/j.nucengdes.2009.10.028

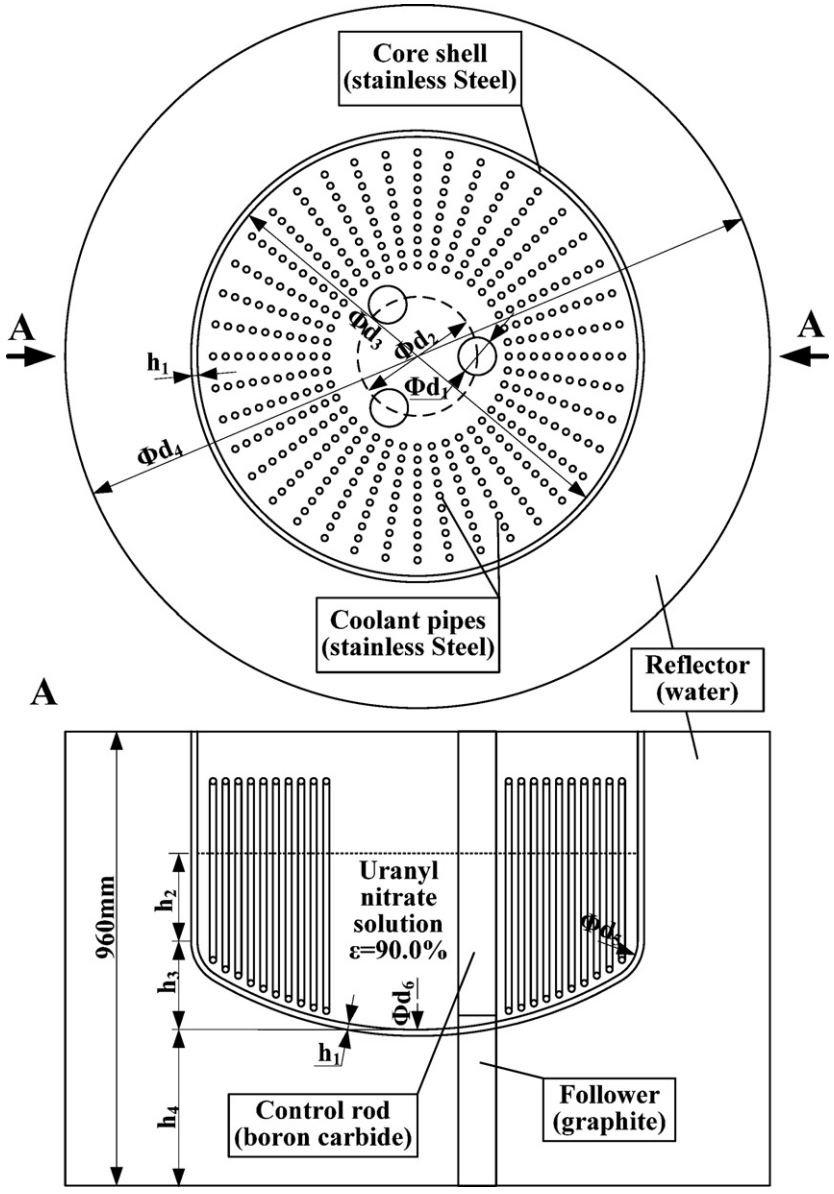

Fig. 1. Structure and materials of the solution reactor.

2.1. Few-group constants calculation

In this section, firstly we select some typical core states with different burnups, void fractions and power levels. For example, the power could be 20% FP (Full Power), 60% FP, 100% FP, 140% FP and 180%FP. Then, for each state, homogenization calculation, as shown in Fig. 3, will be carried out to get macroscopic few-group-few-region constants. There are many differences in few-group constants calculation between aqueous homogeneous solution reactors and traditional reactors (Peng, 2008). Here we only discuss three main aspects of them, which are resonance calculation, depletion calculation and few-group constants fitting.

2.1.1. Resonance calculation

Homogeneous resonance approximation is adopted in FMSR for three reasons. First, the main material in the reactor core is homogenous aqueous fuel solution, whose volume ratio in active core is more than 90%. Second, the rest ingredients are mainly water, whose moderation characteristic is similar to aqueous solution. Third, neutron moderation is sufficient in aqueous solution reactors, which makes the cross-sections of resonance nuclide in resonance energy groups change slowly in terms of diluted cross-section. Therefore, the difference caused by homogenous resonance calculation will be acceptable.

2.1.2. Depletion calculation

In order to calculate the effect of nuclide depletion on group constants, we need to know nuclides-densities variation with time. Since the fuel solution flows and mixes incessantly, nuclides distribution in fuel solution is nearly flat. So the point depletion approximation can be used, in which depletion equations without spatial variable are solved. The depletion calculation is solved by implicit difference method, described as:

$$N^{(k+1)} = N^{(k)} + \frac{\Delta t_k}{2}(f^{(k)} + f^{(k+1)}) \quad (1)$$

where

$$N^{(k)} = (N_1^{(k)}, \ldots, N_m^{(k)}, \ldots, N_M^{(k)})^T$$

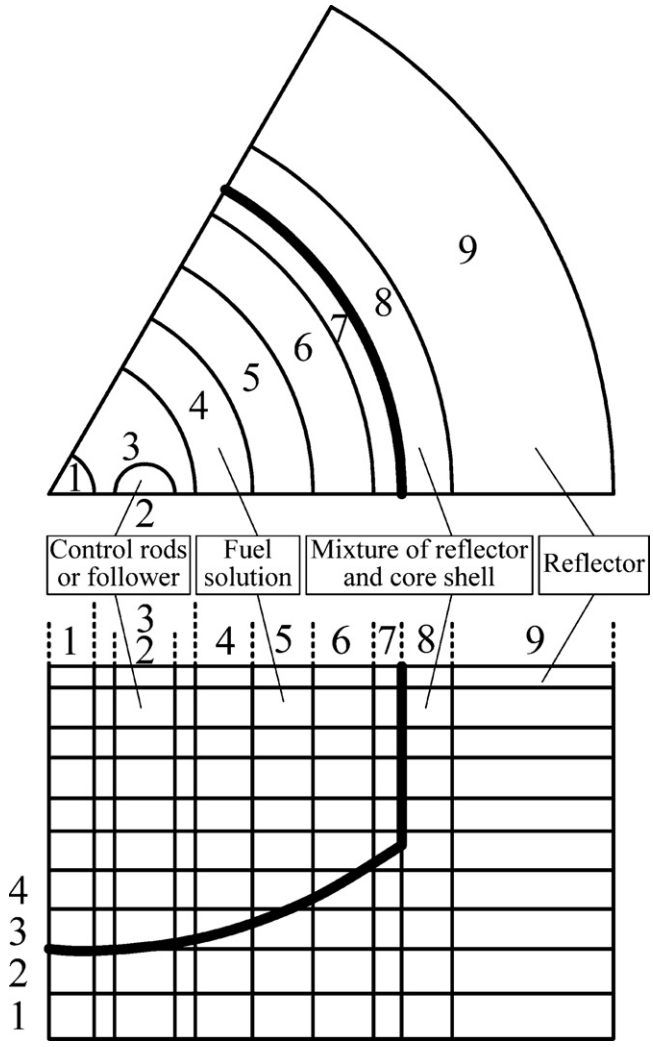

Fig. 2. In-core regions compartmentalization.

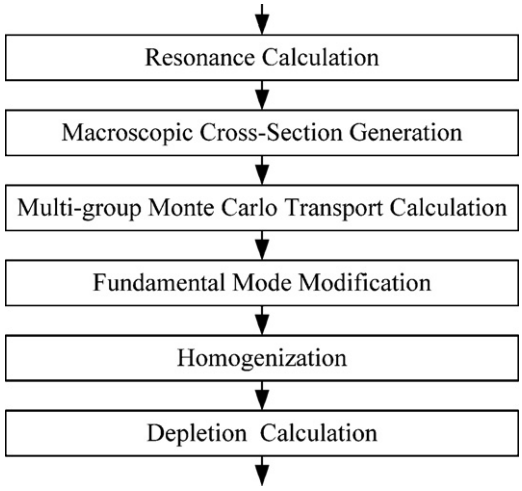

Fig. 3. Calculation for homogenization few-group constants.

$$f^{(k)} = \left(\frac{dN_1^{(k)}}{dt}, \ldots, \frac{dN_m^{(k)}}{dt}, \ldots, \frac{dN_M^{(k)}}{dt} \right)^T$$

The nuclides densities are got by prediction–correction algorithm, which can be described by Fig. 4.

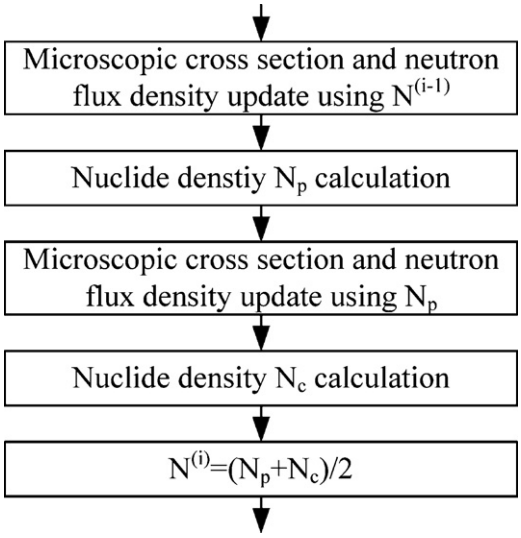

Fig. 4. Prediction–correction in depletion calculation.

2.1.3. Few-group constants fitting

The few-group constants are fitted into the following form:

$$\Sigma_x = f_1(\mathrm{Bu}) f_2(v) f_3(p) + f_4(\mathrm{Bu}) \cdot \delta(\mathrm{Cr}) \quad (2)$$

where $f_i(x)$ ($i = 1, 2, 3, 4$)is a polynomial of variable x; δ(Cr) the Dirac function which equals to 1 or 0 when control rods exist or not; Bu the burnup (MW × d/tU); v the void fraction; and p the relative power.

In the fitting process, some special technologies are taken in order to ensure a high precision. For example, burnup is divided into several sections and fitting calculations are carried out in each section.

2.2. In-core fuel management calculation

In the in-core fuel management calculation, the variation of the core was predicted for a series of time steps, so the whole operation history of a reactor can be simulated. According the actual operation process of aqueous solution reactors, FMSR can perform four main calculations. The code could search the critical core state by moving the control rods, see Fig. 5 in detail; could provide all the kinetic parameters needed by transient code; could simulate the

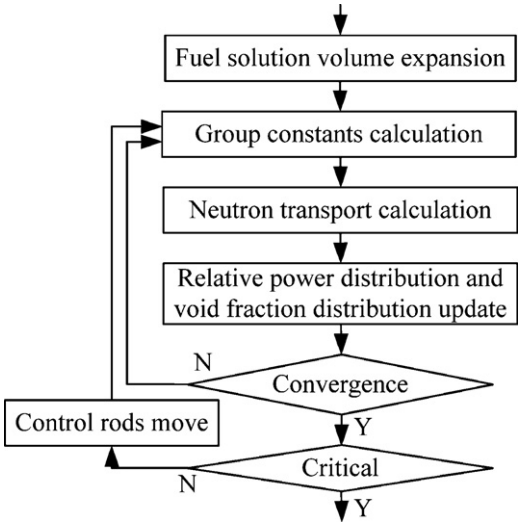

Fig. 5. Critical state searching.

Table 1
Void bubble parameters.

Parameter	Value	Parameter	Value
$G(H_2)$	$3.75 \times 10^{+16}\,J^{-1}$	r_B	0.5 μm
ξ	2	σ	0.075 kg s^{-1}
T_g	500 K	τ_B	8.73 s

shutdown state of the reactor and calculate the shutdown margin; could simulate the isotopes distillation.

There are some differences in the in-core fuel management calculation between solution reactors and traditional solid ones, such as neutron transport calculation, void bubbles calculation, depletion calculation, and so on.

2.2.1. In-core neutron transport calculation

As the aqueous homogeneous solution reactor is a small reactor with strong anisotropic scattering materials and complex geometry, traditional in-core diffusion calculation is not applicable. Three-dimensional neutron transport calculation for unstructured-meshes should be adopted. In this study, the 3D neutron transport solver DNTR (Lu, 2007), which is based on a discrete ordinates node method in triangle-z meshes, is employed for the in-core neutron transport calculation. In this method, general triangles are transformed into an equilateral triangle using the area coordinates. Then the transverse integration technique is done on the equilateral triangles. Multi-group reactor core/criticality problems can be solved accurately and effectively by the solver DNTR.

2.2.2. Void bubbles and fuel solution volume expansion

In aqueous homogeneous solution reactors, void bubbles affect the core state by changing the density and volume of fuel solution. The change of fuel solution density is considered by interpolating macroscopic cross-sections in terms of void fraction, while the volume change of fuel solution is considered by modifying the height of fuel solution surface.

In the volume calculation of void bubbles, the total void volume is given by (Souto et al., 2005):

$$\bar{V}_B = \left(1 + \frac{1}{\xi}\right) \frac{G(H_2)}{N_A} R_g T_g \left(\frac{r_B}{2\sigma}\right) \tau_B \cdot \bar{n} \tag{3}$$

where $\bar{V}_B$ is the total void volume (m^3); $\bar{n}$ is the reactor power (MW); $G(H_2)$ is the hydrogen yield in fuel solution (J^{-1}); ξ is the fraction of H_2 molecules per O_2 molecule produced by water radiolysis; N_A is the Avogadro's constant ($6.0221415 \times 10^{+23}$ mol^{-1}); R_g is the gas constant (8.3143 J mol^{-1} K^{-1}); T_g is the void bubble temperature (K); r_B is the void bubble characteristic radius (μm); σ is the fuel solution surface tension (kg s^{-1}); and τ_B is the characteristic time for void bubble release from the fuel solution (s).

These parameters' values are listed in Table 1 (Souto et al., 2005). Here all types of gas in the bubble with different composition can be considered by choosing different ξ. In Table 1, for example, $\xi = 2$ means the stoichiometric composition ratio between H_2 and O_2 is 2:1.

Actually, the distribution of void bubbles is stochastic. In this paper, we just focus on the mean value because the volume of the fictive assembly is huge enough compared with the volume of the gas bubbles. In addition, the distributions of void bubbles in radial direction and in axial direction are different. In radial direction, void distribution is decided by radial power distribution; while in axial direction by the law of axial void movement. In this paper, we suppose that void distribution in axial direction obeys integral power distribution.

Fuel solution volume expansion is caused by generation of void bubbles and thermal expansion and contraction of the fuel solution.

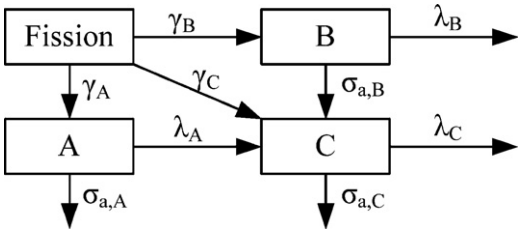

Fig. 6. Simplified isotopes depletion process in fission reactors.

The increment of the fuel solution volume can be determined by:

$$\Delta V = V_{Void} + \Delta V_{Hot} = V_{Void} + \left(\frac{\rho_{Cold}}{\rho_{Power}} - 1\right) \cdot V_{Cold} \tag{4}$$

where V_{Void} is the total void volume (cm^3); ΔV_{Hot} is the solution volume increment caused by thermal expansion and contraction (cm^3); ρ_{Cold} is the density of cold solution (g/l); ρ_{Power} is the density of hot solution (g/l); and V_{Cold} is the volume of cold solution (cm^3).

2.2.3. Depletion calculation

In aqueous homogeneous solution reactors, the changes of nuclide densities will affect macroscopic few-group constants. Most of them can be decided by burnup except two kinds of isotopes. Ones are distilled isotopes, because it is unpredictable that when and how much of the isotopes will be distilled. The others are poisons, including ^{135}Xe and ^{149}Sm, because their nuclide densities will be decided by the idiographic operation process of the reactor.

In a fission reactor, the depletion processes of fission product isotopes can be described by transmutation-decay chain as shown in Fig. 6.

And the depletion equation can be written as follows:

$$\begin{cases} \dfrac{dN_A}{dt} = b_A - a_A N_A \\ \dfrac{dN_B}{dt} = b_B - a_B N_B \\ \dfrac{dN_C}{dt} = b_C + \lambda_A N_A + R^B_{m.a} N_B - a_C N_C \end{cases} \tag{5}$$

where $b_X = \gamma_X R_f$ is the generation rate from fission of isotope X (A, B, C) (s^{-1} cm^{-3}); $a_X = R^X_{m.a} + \lambda_X$ is the decrease rate coefficient of isotope X (s^{-1}); R_f is the macroscopic fission nuclear reaction rate of isotope X (s^{-1} cm^{-3}); $R^X_{m.a}$ is the microscopic absorption nuclear reaction rate of isotope X (s^{-1}).

If initial nuclide densities were ascertained, the solution can be written as follows:

$$\begin{cases} N_A(t) = \left(N_A(0) - \dfrac{b_A}{a_A}\right) e^{-a_A t} + \dfrac{b_A}{a_A} \\ N_B(t) = \left(N_B(0) - \dfrac{b_B}{a_B}\right) e^{-a_B t} + \dfrac{b_B}{a_B} \\ N_C(t) = \left(N_C(0) - \dfrac{b_C}{a_C}\right) e^{-a_C t} + \dfrac{b_C}{a_C} + \dfrac{\lambda_A}{a_C - a_A}\left(N_A(0) - \dfrac{b_A}{a_A}\right)(e^{-a_A t} - e^{-a_C t}) \\ \quad + \dfrac{R^B_{m.a}}{a_C - a_B}\left(N_B(0) - \dfrac{b_B}{a_B}\right)(e^{-a_B t} - e^{-a_C t}) + \dfrac{1}{a_C}\left(\dfrac{\lambda_A b_A}{a_A} + \dfrac{R^B_{m.a} b_B}{a_B}\right)(1 - e^{-a_C t}) \end{cases} \tag{6}$$

The distillation process of isotope X can be written as:

$$N_{X,1} = (1 - per_X) \cdot N_{X,0} \tag{7}$$

where per_X is the distillation ratio of isotope X given by user; $N_{X,0}$ ($N_{X,1}$) is the nuclide density of isotope X before (after) distillation.

These isotopes, except ^{135}Xe, distribute evenly in the fuel solution since they flow together with fuel solution in the container. ^{135}Xe is gas poison and will escape from the fuel solution. So in radial direction, distribution of ^{135}Xe is decided by radial power distribution when the reactor is on power operating, and is uniform when the reactor is shut down. And in axial direction, distribution of ^{135}Xe is decided by the law of void bubbles movement in axial

Table 2
Geometry sizes of the solution reactor.

Label	Value (mm)	Label	Value (mm)
h_1	10	h_2	140
h_3	131.1	h_4	260
d_1	60	d_2	190
d_3	700	d_4	1120
d_5	126	d_6	1260

Table 3
Geometry sizes of the two critical assemblies.

Label	Value (mm)		Label	Value (mm)	
	Assy. 1	Assy. 2		Assy. 1	Assy. 2
h_1	5	5	h_2	139.757	175.761
h_3	106.15	106.15	h_4	222	222
d_1	–	44	d_2	–	250
d_3	550	550	d_4	1290	1290
d_5	11	11	d_6	1100	1100

direction. In this paper, we suppose that the axial distribution of isotope ^{135}Xe is the same as the void bubbles.

3. Numerical results

The calculation model described above has been implemented in the code FMSR. This code is verified against two critical assemblies. The k_{eff} and the control rods worth of solution reactor under cold state were compared with reference results. All these reference results are calculated by MCNP, a Monte Carlo program (Briesmeister, 2002). In the in-core calculation of these results, the whole bottom reflector (h_4 in Fig. 1 and Table 2) is considered and the number of axial layer is 15. FMSR can give relative power distribution, void fraction distribution, cycle length, reactivity feedback coefficients, nuclides densities of poisons and distilled isotopes. Since we have no codes available for the calculation of aqueous homogenous solution reactor in hot state or any measured value, the results of solution reactor in hot state are given without reference results. In the in-core calculation of these results, only 30 mm bottom reflector is considered and the number of axial layer is 10.

The fuel solution of the aqueous homogeneous solution reactor we studied is uranyl nitrate with mass concentration 8.7% and cold state temperature 300 K, in which the uranium enrichment at BOL is 90%. And the actual power of the reactor is 0.2 MW. The size is given by Table 2. Furthermore, 4-group constants are used in all these calculations.

3.1. Critical assembly validation

Two critical assemblies, which have the same structure with the aqueous homogeneous solution reactor except their sizes showed in Table 3, are given for test. In assembly 1, there are no control rods and coolant pipes; the temperature of the materials is 283.35 K; the mass concentration of the fuel solution is 7.3% and the density 1.0549 g/cm^3. In assembly 2, the temperature is 292.5 K; the mass concentration of the fuel solution is 7.3% and the density 1.0557 g/cm^3; all the three control rods are fully withdrawn with two of them filled by the followers and the other one by air (which can be replaced by a follower in calculation). Table 4 shows the results in which the maximal error is less than 0.15%.

Table 4
k_{eff} calculations of critical assemblies.

	Assembly 1	Assembly 2
k_{eff}	0.9997123	0.9985107
Error	0.029%	0.149%

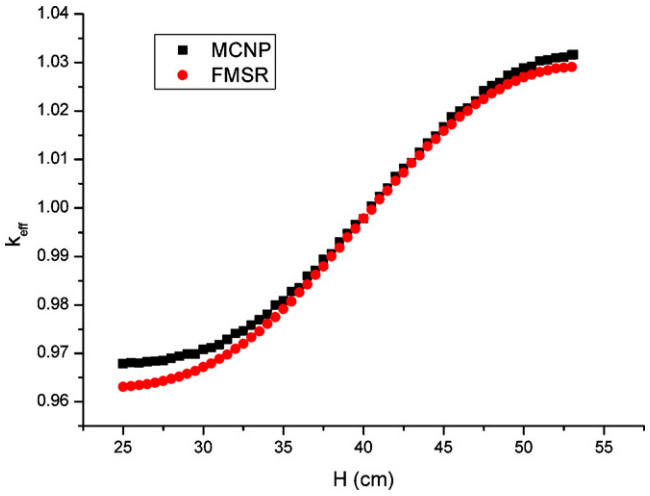

Fig. 7. k_{eff} variations with control rods position.

Table 6
Relative power distribution.

	1	3	4	5	6	7
9	0.896	0.743	0.631	0.537	0.397	0.279
8	1.483	1.211	1.013	0.853	0.624	0.437
7	2.155	1.749	1.395	1.150	0.827	0.572
6	2.718	2.261	1.640	1.309	0.917	0.623
6	2.970	2.478	1.699	1.314	0.893	0.598
5	3.001	2.470	1.630	1.222	0.810	0.448
4	2.804	2.268	1.449	1.065	0.445	0.005
3	2.390	1.909	1.212	0.517	0.006	0
2	1.882	1.083	0.204	0	0	0

3.2. Control rods worth of solution reactor

Table 5 gives the comparison of numerical results of k_{eff} between FMSR and MCNP, and Fig. 7 shows the comparison of k_{eff} variation with control rods' heights calculated by the two programs. All these results are calculated for the cold state of aqueous homogenous solution reactor. In the MCNP calculation, 8,000,000 histories with 500 cycles including 100 inactive cycles were run. In Fig. 7, the maximum relative error is 0.50% which happens when control rods height is 25.0 cm. The results show that the accuracy of FMSR is acceptable in engineering, and the differences between 1/6 core calculations and the whole core ones are very small.

Table 5
Comparison of k_{eff} between FMSR and MCNP.

CRs position	MCNP		FMSR			
	k_{eff}	Standard deviation	1/6 core		Whole core	
			k_{eff}	Error	k_{eff}	Error
In	0.96786	0.00027	0.96307	0.50%	0.96300	0.50%
Out	1.03163	0.00027	1.02936	0.22%	1.02934	0.22%

Table 7
Factors of the power distribution.

Name	Value
The peaking factor	3.001
The radial peaking factor	2.242
The axial peaking factor	1.328
The axial offset factor	0.042

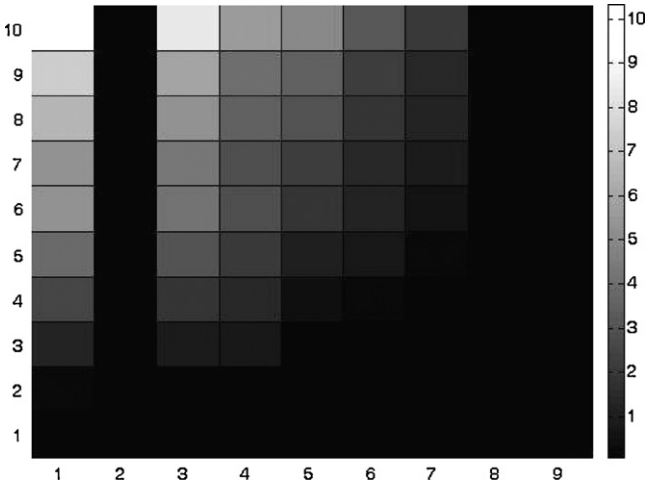

Fig. 8. Void fraction (%) distributions.

3.3. Relative power distribution

Table 6, in which abscissa means radial region No. and ordinate means axial layer No., gives the relative power distribution in a critical core of aqueous homogeneous solution reactor with control rods in layers from 8 to 10 and follower in layers from 1 to 7. The regions with radial number 2, 8 or 9, or axial number 1, are omitted, because they are non-fissile regions. Table 7 gives the factors of the power distribution. And Fig. 8, in which abscissa is radial region No. and ordinate is axial region No., gives the void fraction distribution.

3.4. Cycle length

Fig. 9 gives the in-core k_{eff} variations with core lifetime EFPD (Effective Full Power Day) with all control rods fully withdrawn. At the beginning, k_{eff} drops sharply because of the accumulating of ^{135}Xe in the first 2 days. After that, k_{eff} declines linearly because of the decrease of fissile isotopes and the increase of ^{149}Sm.

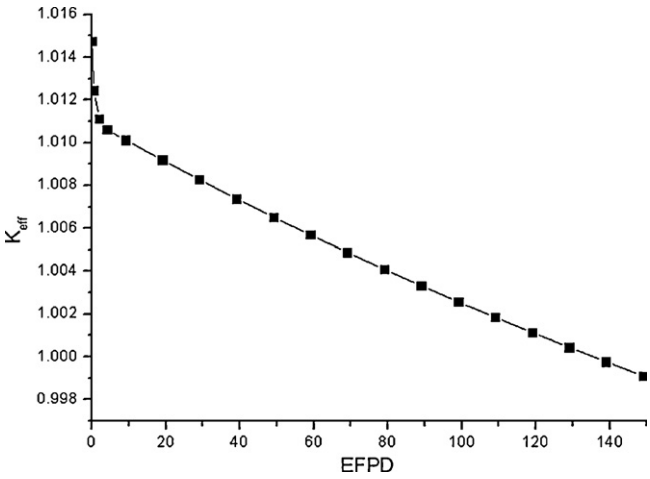

Fig. 9. k_{eff} variation with EFPD.

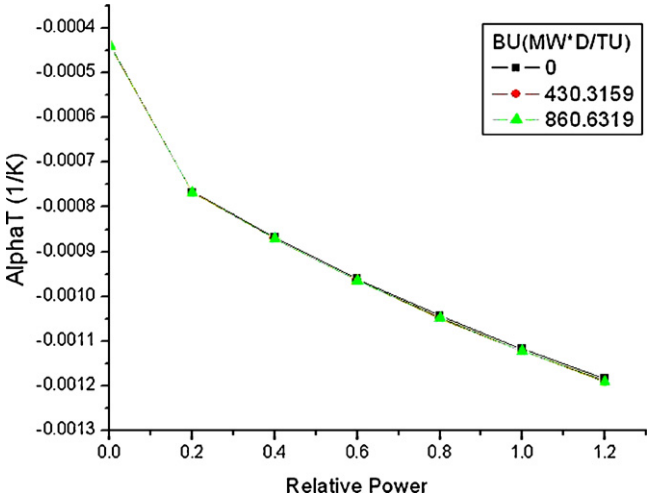

Fig. 10. Temperature coefficient of reactivity.

3.5. Reactivity feedback coefficients

Figs. 10 and 11 show the temperature and void coefficients of reactivity variations with relative power and burnup. From the two figures, we can find both of those two reactivity feedbacks are negative, and the higher the relative power is, the stronger the feedbacks are. This phenomenon can be explained as following. Firstly, the power distribution tends to be flatter in higher power level. Because the increasing power will cause the increasing temperature and void fraction, both of which will cause the expansion of fuel solution. In addition, large void fraction and higher temperature appear where power density is larger. All these factors make the power distribution flatter. Second, in a core with flatter power distribution, the negative feedback effect works more efficiently in a wider range. Consequently, the feedbacks will be stronger.

3.6. Nuclides densities of poisons and distilled isotopes

In order to simulate fuel management process, Fig. 12 gives relative power variation with the time in a stop-restart process. In this process, isotopes are distilled when the reactor is shut down, and the distillation proportions are listed in Table 8.

Nuclide-densities variations are showed in Figs. 13–15. In Fig. 13, the density of ^{127}I increases linearly when reactor is on

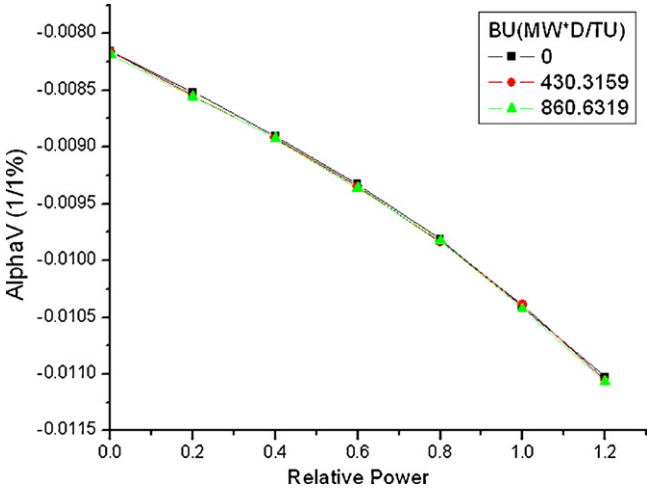

Fig. 11. Void fraction coefficient of reactivity.

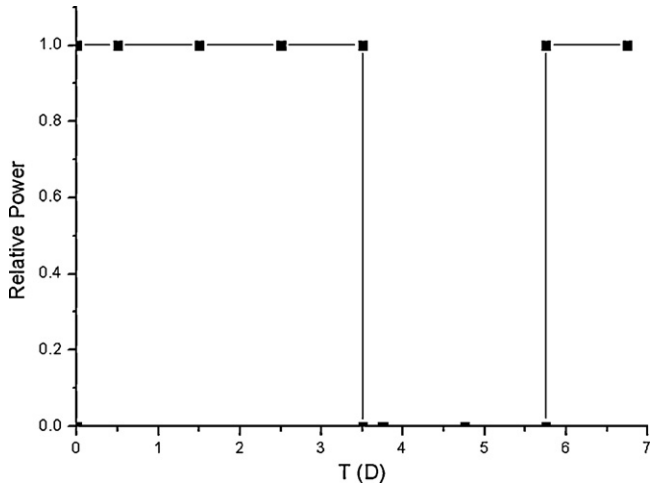

Fig. 12. Relative power variation.

Table 8
Isotopes distillation proportions.

Isotope	Proportion
^{127}I	60%
^{149}Pm	30%
^{149}Sm	30%

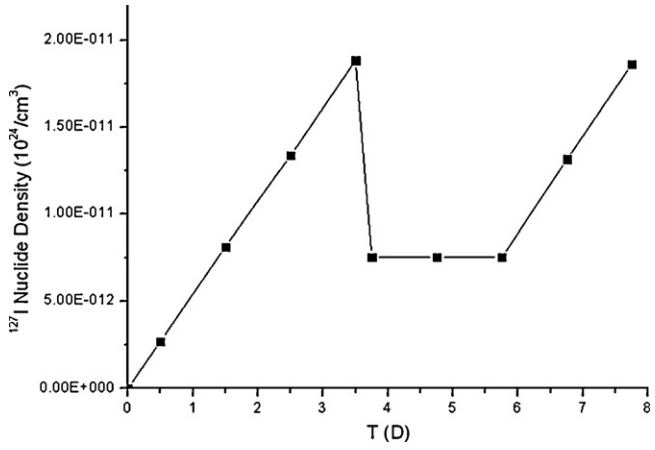

Fig. 13. Density variation of ^{127}I.

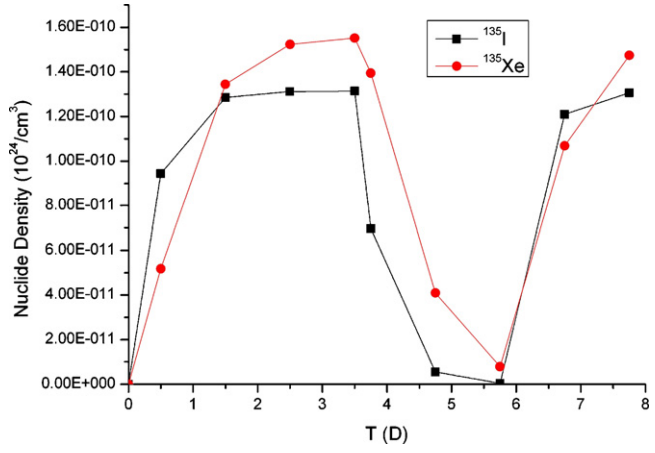

Fig. 14. Density variations of ^{135}I and ^{135}Xe.

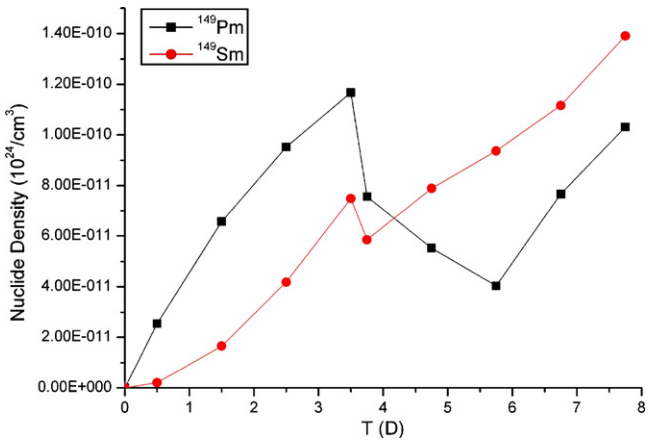

Fig. 15. Density variations of ^{149}Pm and ^{149}Sm.

power operating; while keeps changeless when shut down, since it is stable isotope. On the contrary, isotopes ^{135}I, ^{135}Xe, ^{149}Pm and ^{149}Sm are unstable ones. And their densities come to their saturation states in an exponential law when reactor is on power operating; while decrease because of self-decay or increase because of the decays of their precursors when reactor is shut down, as shown in Figs. 14 and 15.

Flux densities in the aqueous homogeneous solution reactors are so low that some characteristics are noticeable in Figs. 14 and 15. Firstly, the saturation density of ^{135}I is smaller than ^{135}Xe. The proportion of these two saturation densities can be written as follow:

$$\frac{N_{\mathrm{I}}(\infty)}{N_{\mathrm{Xe}}(\infty)} = \frac{\lambda_{\mathrm{Xe}} + \sum_{g=1}^{G}\sigma_{a,g}^{\mathrm{Xe}}\phi_g}{\lambda_{\mathrm{I}} + (y^{\mathrm{Xe}}/y^{\mathrm{I}})\cdot\left(\lambda_{\mathrm{I}} + \sum_{g=1}^{G}\sigma_{a,g}^{\mathrm{I}}\phi_g\right)} \approx \frac{y^{\mathrm{I}}}{(y^{\mathrm{I}}+y^{\mathrm{Xe}})\cdot\lambda_{\mathrm{I}}}\cdot\left(\lambda_{\mathrm{Xe}} + \sum_{g=1}^{G}\sigma_{a,g}^{\mathrm{Xe}}\phi_g\right) \quad (8)$$

When the average flux density is less than a certain level, this proportion will be less than 1.0. Second, iodine pit does not appear as anticipated. The appearance of iodine pit is characterized by:

$$N_{\mathrm{Xe}} \le \frac{\lambda_{\mathrm{I}}}{\lambda_{\mathrm{Xe}}}\cdot N_{\mathrm{I}} \quad (9)$$

which will be satisfied only when the average flux density is higher than a certain level. Third, saturation ^{149}Sm poisoning period is much longer than the one in pressure reactor, because the period:

$$t \gg \left(\sum_{g=1}^{G}\Sigma_{a,g}^{\mathrm{Sm}}\phi_g\right)^{-1} \quad (10)$$

increases as the average flux density decreases.

4. Conclusion

Aiming at the fuel management calculation of aqueous homogeneous solution reactors, this paper establishes calculation models and develops an in-core fuel management calculation code FMSR. Numerical results show that the maximum relative error of k_{eff} for static state compared with MCNP is less than 0.5%. The code FMSR can be used in fuel management calculation of aqueous homogeneous solution reactors as a trial. However, the program still needs more validations, especially for the hot state, because of the lack of experimental data at present.

Acknowledgment

This work is supported by the National Natural Science Foundation of China grants no. 10605017 and 10875094, and also supported by the International Atomic Energy Agency under the Coordinated Research Project (contract no.: CRP15009).

References

Ball, R.M., 1997. Medical Isotope Production Reactor [P]. US: 5596611.
Briesmeister, J.F., 2002. MCNP-A General Monte Carlo N-Particle Transport Code, Version 4C, LA-13709-M.
Dunenfeld, M.S., Stitt, R.K., 1963. Summary Review of the Kinetics Experiments on Water Boilers. NAA-SR-7087. Atomics International.
Lecorche, P., Seale, R.L., 1973. Review of the Experiments Performed to Determine the Radiological Consequences of a Criticality Accident. Y-CDC-12. Oak Ridge National Laboratory.
Lu, H., 2007. Nodal methods for the neutron diffusion and transport equations in triangular meshes. Ph.D Thesis. Xi'an Jiao Tong University, China.
Malenfant, R.E., Forehand, H.M., Koelling, J.J., 1980. Sheba: a solution critical assembly. Trans. Am. Nucl. Soc. 35, 279–280.
Peng, S., 2008. The few-group cross-sections calculation method of medical isotope production reactor. Master Thesis. Xi'an Jiao Tong University, China.
Souto, F.J., Kimpland, R.H., Heger, A.S., 2005. Analysis of the effects of radiolytic-gas bubbles on the operation of solution reactors for the production of medical isotopes. Nucl. Sci. Eng. 150, 322–335.